| Title | Transitory memory retrieval in a biologically plausible neural network model |
|---|---|
| Author(s) | , |
| Citation | . ( ) 6884 |
| Issue Date | 2013-06-28 |
| DOI | 10.14943/doctoral.r6884 |
| Doc URL | http://hdl.handle.net/2115/53212 |
| Type | theses (doctoral) |
| File Information | Hiromichi_Tsukada.pdf |

Instructions for use

# Transitory memory retrieval in a biologically plausible neural network model

2013

Hiromichi Tsukada

Department of Mathematics, Graduate School of Science

Hokkaido University

## Abstract

A number of memory models have been proposed. These all have the basic structure that excitatory neurons are reciprocally connected by recurrent connections together with the connections with inhibitory neurons, which yields associative memory (i.e., pattern completion) and successive retrieval of memory. In most of the models, a simple mathematical model for a neuron in the form of a discrete map is adopted. It has not, however, been clarified whether behaviors like associative memory and successive retrieval of memory appear when a biologically plausible neuron model is used. In this paper, we propose a network model for associative memory and successive retrieval of memory based on Pinsky-Rinzel neurons. The state of pattern completion in associative memory can be observed with an appropriate balance of excitatory and inhibitory connection strengths. Increasing of the connection strength of inhibitory interneurons changes the state of memory retrieval from associative memory to successive retrieval of memory. We investigate this transition.

## Keywords

## Contents

# List of Figures

# 1 Introduction

Several models for assocative memory have been proposed so far, which have the basic structure that excitatory neurons are reciprocally connected by recurrent connections. This structure yields associative memory, that is, pattern completion [1-5]. An extended model of associative memory by introducing additional inhibitory interneurons, which treats successive retrieval of memory, has also been proposed [6-8].

On the other hand, it has become possible to introduce the effects of ion channels, neuromodulators, and the geometric structure of synaptic connections, based on biological knowledge of neuronal activity that has recently accumulated. For example, each area of a dendrite receives glutamatergic inputs from a different source, and several types of interneurons connect with different areas of a dendrite [9-11]. However, it has not been clarified how these factors contribute to the memory system. Therefore, in order to construct a memory model consisting of biologically plausible neuron units, it is necessary to use a conductance-based model, which includes ion channels, membrane dynamics, and the geometric structure of synaptic connections. By using this level of model, we consider the effects of the factors mentioned above. We believe that this level of modeling could link computational theory with physiological data. In other words, our present approach in terms of mathematical modeling corresponds to the intermediate level of theory proposed by D. Marr [12], that is, "representation and algorithm". Here we focus on a conductance-based model of associative memory.

Furthermore, based on physiological experiments, it has been reported that Acetylcholine (ACh) projection reduces the release of GABA, and hence decreases IPSPs in pyramidal cells of layer 2/3 in the cerebral cortex [13-15]. This indicates that ACh projection modulates the GABAergic synaptic property. Interneurons modulate and coordinate the firing patterns of pyramidal cells, and stabilize the activity of pyramidal cells by both feedback and feedforward inhibitions [9, 16]. If the synaptic currents from GABAergic interneurons to pyramidal cells are modulated by ACh

1

projections, the firing pattern of pyramidal cells would also be changed. Therefore, we assume that the state of memory retrieval should be closely related to such ACh projections.

In this study, focused on these effects of ACh, we also describe the relationship between associative memory and successive retrieval of memory.

## 2 Model

### 2.1 Network architecture

The network architecture in our model is a population of pyramidal cells that are reciprocally connected by recurrent connections and GABAergic fast-spiking interneurons. These interneurons project via $GABA_A$ synapses to pyramidal cells, and the pyramidal cells project via AMPA synapses to other pyramidal cells forming a recurrent network and also project via AMPA synapses to interneurons. We do not include effect of NMDA channels because we do not consider synaptic learning directly. The network is composed of 150 neurons: 120 pyramidal cells (80%) and 30 interneurons (20%). Three memory patterns, provided as binary patterns, are embedded into the recurrent excitatory synaptic connections by Hebbian synaptic modification. The Hebbian rule specifies a weight of 1 for a connection between two active neurons and otherwise a weight of zero (see Appendix C for details). The dendritic compartment receives the spike trains of external inputs and background noise, the latter being independently generated by a Poisson process with an average 1 kHz firing rate. The schematic network architecture is shown in Fig. 1, and the mathematical representation appears in Appendices A-C.

### 2.2 Pyramidal cells

We employ a two-compartment model for pyramidal cells that was proposed by Pinsky and Rinzel [17]. It consists of somatic and dendritic compartments comprising different active ion-currents and synaptic inputs. The somatic compartment has two voltage-dependent currents, the fast sodium current $I_{Na}$ and the delayed rectifier potassium current $I_{K-DR}$, and a leak current $I_L$. The dendritic compartment has three voltage-dependent currents, which are the calcium current $I_{Ca}$, the Ca-activated potassium current $I_{K-C}$, and the potassium after-hyperpolarization current $I_{K-AHP}$, as well as the leak current $I_L$. The compartments are electrically connected via conductance $g_c$. Each pyramidal cell receives somatic inhibition from GABAer-

gic fast-spiking interneurons, and dendritic excitation from other pyramidal cells (recurrent collaterals). See Appendix A for details.

## 2.3 GABAergic FS interneurons

The interneuron model is a compartment with a sodium current, $I_{Na}$, a potassium current, $I_K$, and a leak current $I_L$ [18]. Each GABAergic FS interneuron receives excitatory input from 4 pyramidal cells, and projects via GABA$_A$ synapses to the somatic compartment of all pyramidal cells. See Appendix B for details.
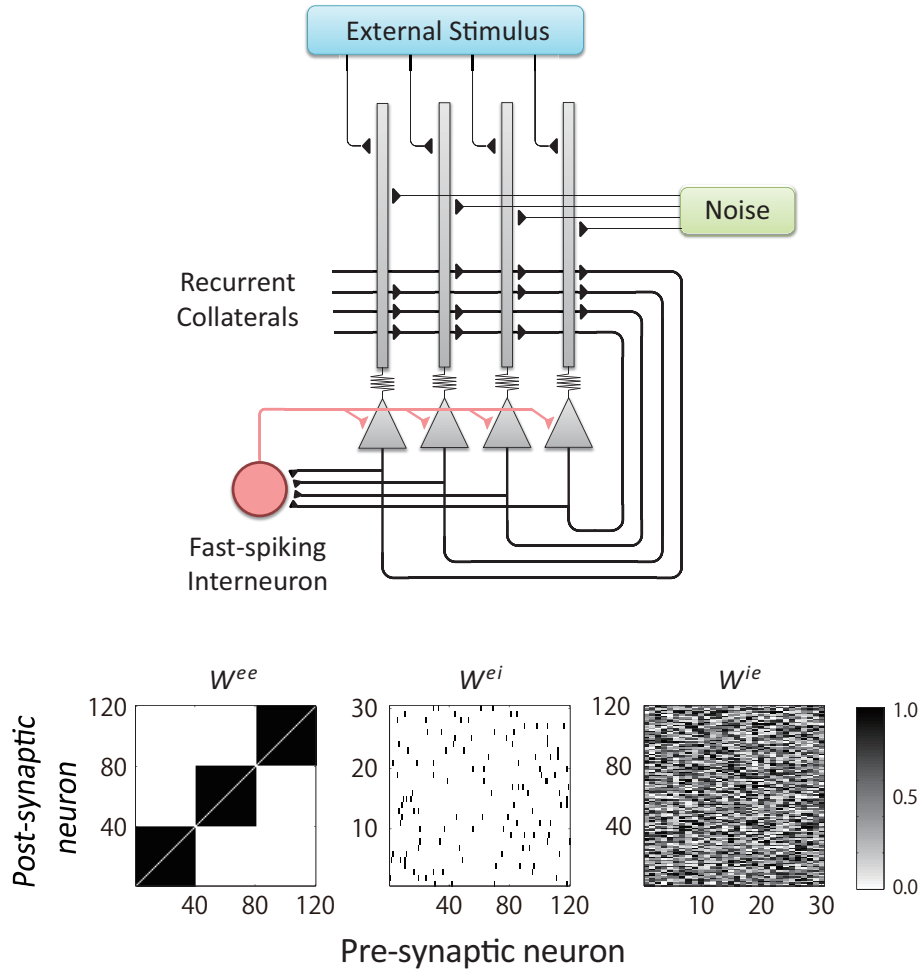


Figure 1: A schematic diagram of the network architecture. The network architecture consists of a population of pyramidal cells which are reciprocally connected by recurrent connections and GABAergic fast-spiking interneurons with external input

4

and noise. Connection matrices and are shown in three columns at the bottom of the figure (see Appendix C for details).

# 3 Results

## 3.1 Dynamic behavior for associative memory

In this section, we investigate whether associative memory is achieved in the Pinsky-Rinzel neurons network. Since the network should have the ability of pattern completion to be associative memory, we evaluate the ability from the network response when a partial cue, which is close to one of stored memory patterns, is applied to the network. The partial cue is produced by reducing the number of active neurons from one of stored memory patterns.

The degree of pattern completion is evaluated by calculating the overlapping $M^\mu$ between the current network state and a stored memory pattern. The overlapping $M^\mu$ is defined by

$$M^\mu = \frac{\eta^\mu \cdot X[k]}{\|\eta^\mu\|\|X[k]\|}, \tag{1}$$

where $\eta^\mu$ is the $\mu$-th embedded memory pattern, each of which is represented by a N-dimensional vector of activities of neurons for an N-neuron network. Here, each element of the vector is encoded by 1 (firing state) or 0 (resting state). $X[k]$ is also a N-dimensional vector for an N-neuron network:

$$X[k] = (x_1[k], x_2[k], \cdots, x_N[k])^T. \tag{2}$$

Here $x_i[k]$ is the number of spikes of the $i$-th neuron during the interval $(kT, (k + 1)T)$ and $T = 10$ ms is fixed. The overlapping $M^\mu$ takes the value of 1 when the current network state is the same as the $\mu$-th embedded memory pattern.

Fig. 2 shows the network response when the partial cue was applied to the network as an external stimulus at times of 0 ms, 250 ms, and 500 ms with each application having a duration of 40 ms. It can be seen that even if the external stimulus is slightly different from stored patterns (see Fig. 2 (a)), the activity pattern rapidly converges to the closest stored pattern (see Fig. 2 (c)). This convergence occurs because pyramidal cells participating in the same memory are enhanced by other pyramidal cells by recurrent connections, but another pyramidal cells, which do not belong to the construction of that memory, are suppressed by inhibitory interneurons. This way of memory retrieval provides associative memory via the network's ability to complete patterns, which has been proposed by many researchers, for instance, Amari [1], Anderson [2], Nakano [3], and Hopfield [4]. In the next section, we examine the properties of pattern completion.
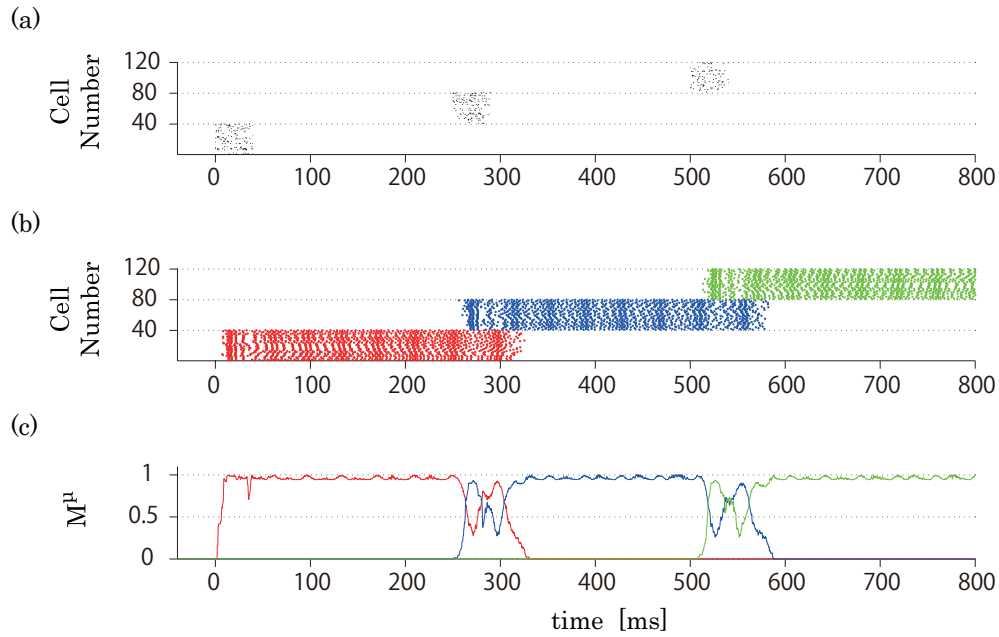


Figure 2: Network response for external stimulation. (a) Rasterplot of external stimulation. A stimulation that was slightly different to the stored pattern was applied to each cell assembly at times 0 ms, 250 ms, and 500 ms, and each stimulus lasted for 40 ms. (b) Rasterplot of somatic spikes. These spikes are induced by the external stimulus inputs. The different colors indicate a different cell assembly. (c) Overlap-

ping between a stored pattern and an activity pattern of the network. Overlapping was calculated using a time window of 10 ms, and the time window for moving average was 0.05 ms. The parameters in this simulation are $g_{GABA} = 0.037$ and $g_{AMPA,rec} = 0.036$. The stimulation suggests that an attractor dynamics emerges and employs auto-association for the recall of memories.

## 3.2   Pattern completion

Pattern completion can be viewed as attractor dynamics and, thus, depends on the structure of basin of attraction of stored patterns. In order to understand the basin structure in phase space, we study the relation between the probability of memory retrieval and the difference between an input pattern and a stored pattern. Input patterns are provided by N-dimensional vectors of binary patterns for an N-neuron network, where each input pattern is provided by increasing or decreasing the number of active neurons from a stored pattern. The difference of the number of active neurons between an input pattern and a stored pattern is defined as DBIS. Plus or minus sign of DBIS indicates the increase or the decrease of the number of active neurons in the input pattern from a stored memory pattern (see Fig. 3 (a)).

The probability of memory retrieval is calculated as follows. An input pattern is selected from the set of input patterns with different DBIS, and applied to the network as an external stimulus at times 50 ms with a duration of 40 ms. Then, the overlapping is calculated from the network response at time of 500 ms after stimulus onset. We define the success of memory retrieval as being greater than 80 % of overlapping. The probability of memory retrieval is calculated as the rate of success of memory retrieval under 40 trials with different initial conditions of the network.

Fig. 3 (b) shows the probability of memory retrieval for different DBIS input patterns. It can be seen the parameter region that accomplish the probability of memory retrieval being almost one, even if the input pattern differs from the stored pattern by several active neurons (see Fig. 3 (b), $g_{GABA} = 0.030$). These results

suggest the presence of attractors in the network dynamics.

Furthermore, this type of memory retrieval becomes unstable with an increase of the connection strength from the inhibitory interneurons to the pyramidal cells, $g_{GABA}$, which indicates that the connection strength could modify the structure of the basin of attraction (see Fig. 3 (b), $g_{GABA} = 0.040$). In the following section, we consider the effect of $g_{GABA}$ in the memory retrieval.
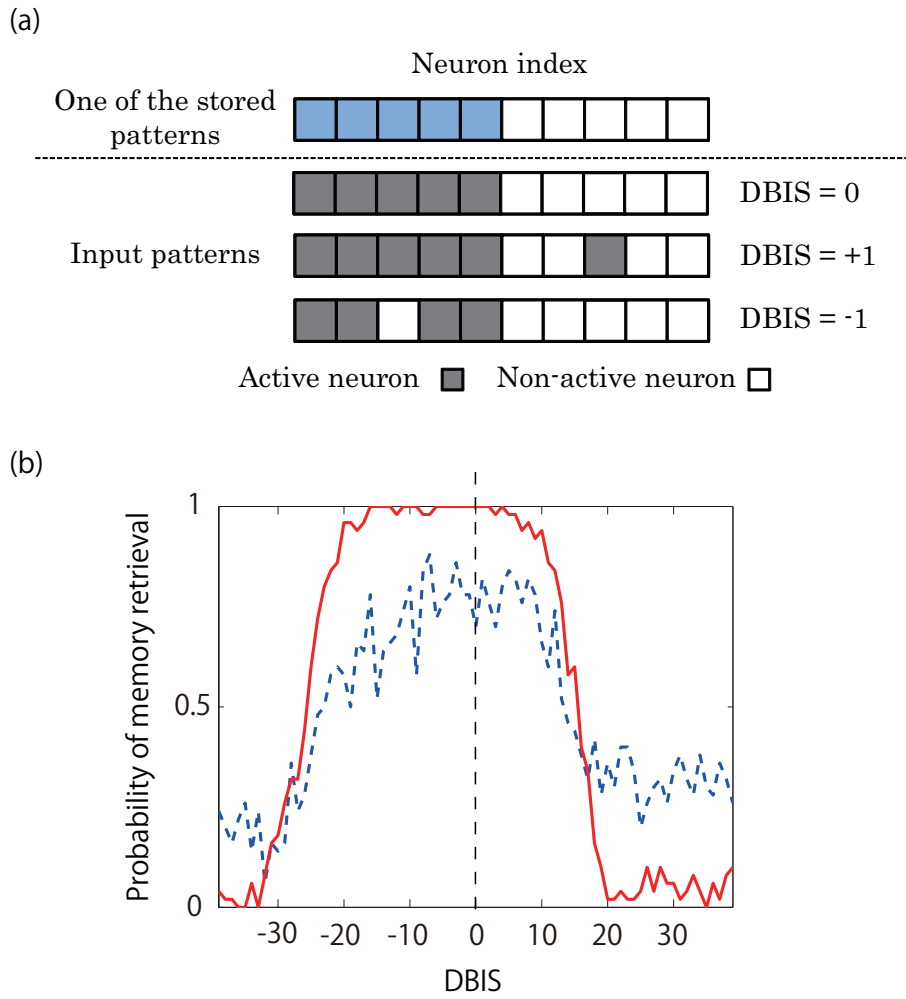


Figure 3: The structure of the basin of attraction. (a) The difference between an input pattern and a stored pattern (DBIS). Plus or minus sign of DBIS indicates the increase or the decrease of the number of active neurons in the input pattern from a stored memory pattern. (b) The abscissa denotes DBIS, and the ordinate denotes the probability of memory retrieval. Red solid and blue dashed curves show the

cases of $g_{GABA} = 0.030$ and $g_{GABA} = 0.040$, respectively.

## 3.3   The influence of inhibition on memory retrieval

We consider the change of dynamics associated with memory retrieval, when the relative strength of inhibitory connections to pyramidal cells changes. Fig. 4 shows a rasterplot of the somatic spikes for all pyramidal cells with different connection strengths $g_{GABA}$ after the input of an external stimulus. Here, the external stimulus is applied at time 0 ms. The connection strength of $g_{GABA}$ starts with $g_{GABA} = 0$ and changes to $g_{GABA} = 0.032$ at 1000 ms, and $g_{GABA} = 0.048$ at 2500 ms (Fig. 4 (a)). Without inhibition, $g_{GABA} = 0$, the firing activity of pyramidal cells is enhanced by recurrent connections, which brings about effects like epileptic seizure (Fig. 4 (b), state I). When $g_{GABA} = 0.032$, the network behaves like associative memory (Fig. 4 (b), state II). When $g_{GABA} = 0.048$, the network state changes dynamically, yielding successive retrieval of memories (Fig. 4 (b), state III). Thus, the modality of the retrieval process changes, depending on the connection strength of GABAergic inhibitory interneurons to pyramidal cells.
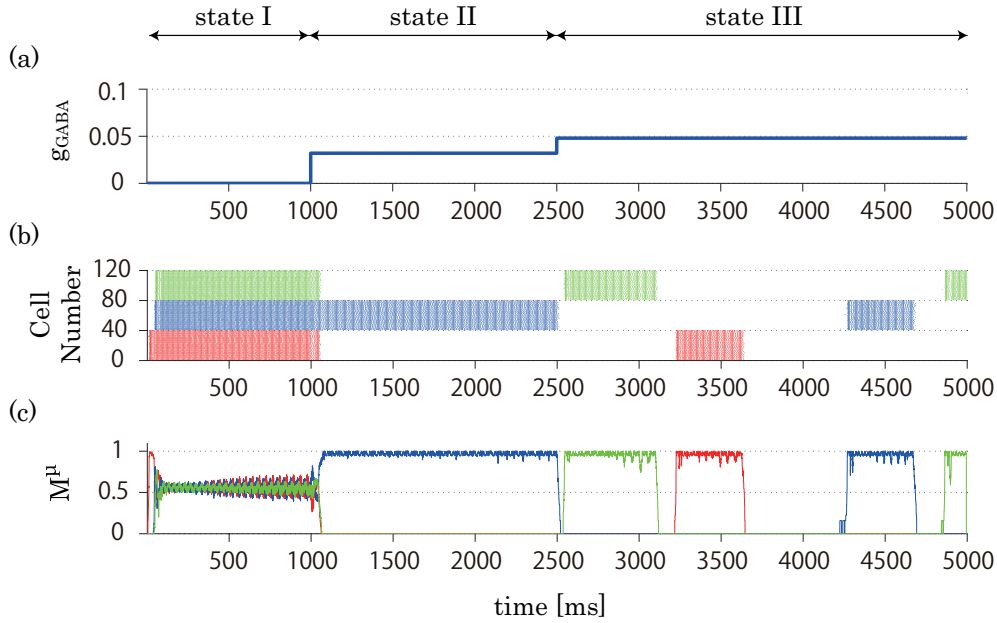


9

Figure 4: Rasterplot of the somatic spikes for different values of the connection strength $g_{GABA}$. We observed the behavior of most cells firing, as in an epileptic seizure, for $g_{GABA} = 0$ (state I), associative memory retrieval for $g_{GABA} = 0.032$ (state II), and successive retrieval of memories for $g_{GABA} = 0.048$ (state III). (a) Time-series of the connection strength $g_{GABA}$. The connection strength starts at $g_{GABA} = 0$, and changes to $g_{GABA} = 0.032$ at 1000 ms, and to $g_{GABA} = 0.048$ at 2500 ms. (b) Rasterplot of somatic spikes. Different colors indicate different cell assemblies. (c) Overlapping between somatic spikes and stored memory patterns.

## 3.4 Effects of $g_{AMPA,rec}$ / $g_{GABA}$ balance for associative memory

We examined the network's ability to behave like associative memory in the parameter space of $g_{AMPA,rec}$ (the strength of excitatory-excitatory connections) and $g_{GABA}$ (the strength of inhibitory connections to pyramidal cells). We performed simulations by fixing DBIS $= -6$ as one of the values in which the pattern completion is accomplished in Fig. 5 (a). We also examined another values, for example, DBIS $= -10, +6$, but there was no essential difference.

We observed that the memory retrieval was successful in the parameter regions of white colored in Fig. 5 (a). This result implies that pattern completion is accomplished for an appropriate balance of $g_{AMPA,rec}$ / $g_{GABA}$ (see Fig. 5 (a) and Fig. 5 (b), state II). In particular, in the parameter region where $g_{GABA}$ is greater than its values by which the pattern completion is accomplished, successive retrieval of memory was observed (see Fig. 5 (b), state III). On the other hand, in the parameter region where $g_{GABA}$ is smaller than its values by which the pattern completion is accomplished, the network behavior such as an epileptic seizure was observed (see Fig. 5 (b), state I). In addition, we labeled "state IV" as the parameter region which could not be classified in any of the three states in Fig. 5 (b). In state IV, various types of complex patterns were observed.
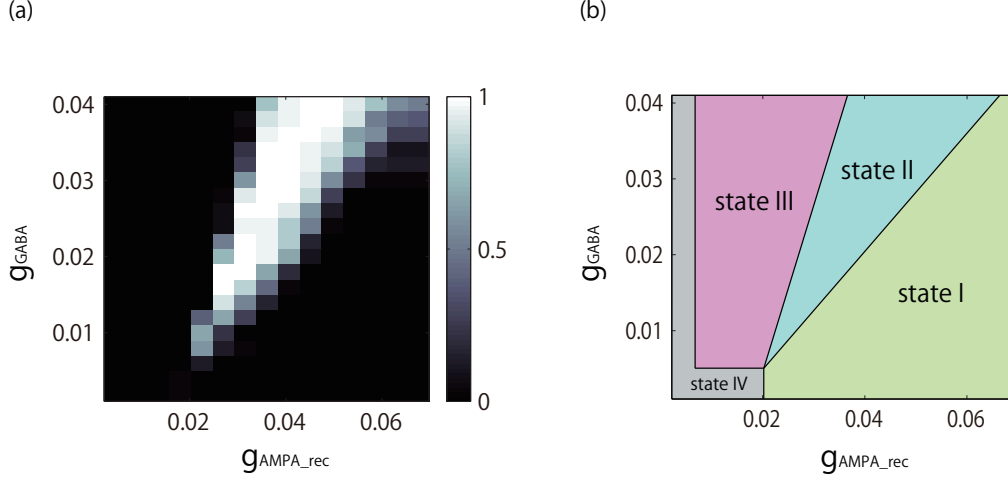
Figure 5: The parameter space of $g_{AMPA,rec}$ / $g_{GABA}$. (a) The difference between the input pattern and one of the stored patterns (DBIS = −6). The white color scale indicates the probability of memory retrieval. (b) The phase diagram of the dynamic states of network: an epileptic seizure (state I), a pattern completion (state II), and a successive retrieval of memories (state III). State IV is a state which could not be classified in any of the above three states.

# 4  Summary and discussion

In this paper, we have proposed a neural network model consisting of biologically plausible Pinsky-Rinzel neuronal units, where the network comprises excitatory recurrent connections and inhibitory connections by GABAergic fast-spiking interneurons.

First, we observed network activity after external stimulus. The activity pattern of the network rapidly converged to one of the stored patterns. This occurred even if the external stimulus was slightly different from the stored pattern. To clarify the network's pattern completion ability, we examined the probability of memory retrieval for different values of the difference between the input and stored patterns. The result suggests that attractor dynamics works in the same way for pattern completion as it does for representing association of memory. The first significant result

of the present study is, therefore, the achievement of an associative memory model in terms of a biologically plausible neural network.

Second, a more dynamic modeling of the process of retrieving memories was also realized in terms of a biologically plausible model. When the relative strength of inhibitory connections to pyramidal cells changes, the basins of attraction of stored patterns are modulated, and thus the retrieval of memory becomes unstable, which gives rise to successive association of memories.

The successive association of memories might be caused by the following two factors. One is the synchronization of interneurons. When strong IPSPs are produced by the synchronization of interneurons, the basin of attraction could be modified and most pyramidal cells could be kicked out of the attractor by noise. Then the memory pattern should disappear. An increase in the degree of synchrony among interneurons could cause transition between memory patterns. The other possibility is the synchronization of pyramidal cells. When pyramidal cells belonging to the same memory synchronize each other, the currents from the recurrent connections flow into their dendrites at the same time. At that time, the reset via absolute refractory period in all pyramidal cells occurs at the same time. Therefore, the pyramidal cells can not keep high in their membrane potential during absolute refractory period, and then stop firing.

With respect to the characteristics of transition among memories, each memory pattern appears in both forms of fixed order and of random order depending on the parameter. In particular, patterns in random order appear in the parameter of boundary area between the states II and III in Fig. 5 (b). In addition, there is the possibility to have the dynamical transitions via NMDA channels. Since NMDA channels on the pyramidal cells have longer time constants than most other channels, say, AMPA channels, the time history of the spikes could be reflected in the membrane potential of pyramidal cells.

This type of successive transition is similar to the behavior of memory retrieval based on chaotic itinerancy [6, 7, 19] or latching dynamics [20]. Clarifying the re-

lationship between the present model and these models is a subject for future study.

Finally, we discuss about the functional role of ACh in memory retrieval. It has been reported that ACh projection reduces the release of GABA, and hence decreases IPSPs in pyramidal cells of layer 2/3 in the cerebral cortex [13-15]. Thus, ACh projection brings about the decrease of the connection strength of $g_{GABA}$ in our model. When the connection strength of $g_{GABA}$ decreases, the network dynamics changes from successive retrieval of memories (state III) to associative memory retrieval (state II) (see Fig. 4). This result suggests the regulations of the process of memory retrieval via ACh projections.

There have been recent findings about the role of ACh on attention mechanisms through its effects on GABAergic interneurons in the physiological experiment. It would be interesting to relate these findings to the change of dynamic modalities of the memory retrieval process in the realistic neural network model studied here. This is a subject for future study.

## Appendix: Model equations

### A: Pyramidal cells

We use a two-compartment model for pyramidal cells proposed by Pinsky and Rinzel [17]. This model consists of somatic and dendritic compartments. The membrane potentials of each compartment are described by

$$C_m \frac{dV_s}{dt} = -g_L(V_s - E_L) - I_{Na} - I_{K-DR} - I_{syn,s} + (g_c/p)(V_d - V_s) + I_s/p,$$

$$C_m \frac{dV_d}{dt} = -g_L(V_d - E_L) - I_{Ca} - I_{K-AHP} - I_{K-C} - I_{syn,d}/(1 - p)$$

$$+ (g_c/(1 - p))(V_s - V_d) + I_d/(1 - p), \tag{3}$$

where the currents are

$$I_{Na} = g_{Na}m_\infty^2(V_s)h(V_s - E_{Na}),$$

$$I_{K-DR} = g_{K-DR}n(V_s - E_K),$$

$$I_{Ca} = g_{Ca}s^2(V_d - E_{Ca}), \tag{4}$$

$$I_{K-AHP} = g_{K-AHP}q(V_d - E_K),$$

$$I_{K-C} = g_{K-C}c \min(Ca/250, 1)(V_d - E_K).$$

The kinetics of gating variables are described by

$$\frac{dx}{dt} = \alpha_x(1 - x) - \beta_x x, \tag{5}$$

where $x$ stands for the different kinetic variables $h$, $n$, $m$, $s$, $c$ and $q$, and $\alpha_x$ and $\beta_x$ are dimensionless time-scales tuning the rate of opening or closing of the channels.

$$\alpha_m = \frac{0.32(-46.9 - V_s)}{\exp((-46.9 - V_s)/4) - 1}$$

$$\beta_m = \frac{0.28(V_s + 19.9)}{\exp((V_s + 19.9)/5) - 1}$$

$$\alpha_n = \frac{0.016(-24.9 - V_s)}{\exp((-24.9 - V_s)/5) - 1}$$

$$\beta_n = 0.25 \exp(-1 - 0.025V_s)$$

$$\alpha_h = 0.128 \exp((-43 - V_s)/18)$$

$$\beta_h = \frac{4}{1 + \exp((-20 - V_s)/5)}$$

$$\alpha_s = \frac{1.6}{1 + \exp(-0.072(V_d - 5))}$$

$$\beta_s = \frac{0.02(V_d + 8.9)}{\exp((V_d + 8.9)/5) - 1}$$

$$\alpha_q = 0.01 \min(Ca/500, 1)$$

$$\beta_q = 0.001$$

$$\alpha_c = \begin{cases} \dfrac{\exp((V_d + 50)/11) - \exp(-(V_d + 53.5)/27)}{18.975} & V_d \leq -10 \\ 2\exp(-(V_d + 53.5)/27) & V_d > -10 \end{cases}$$

$$\beta_c = \begin{cases} 2\exp((V_d + 53.5)/27) - \alpha_c & V_d \leq -10 \\ 0 & V_d > -10. \end{cases}$$

The calcium concentration $Ca$ satisfies

$$\frac{dCa}{dt} = -0.13I_{Ca} - 0.075Ca. \tag{7}$$

The synaptic current $I_{syn}$ is defined below (see Appendix C). We used the following standard values of the parameters for the pyramidal cell. The maximal conductances (in mS/cm$^2$) are $gc = 1$, $g_{Na} = 30$, $g_{K-DR} = 15$, $g_L = 0.1$, $g_{Ca} = 10$, $g_{K-AHP} = 0.8$, and $g_{K-C} = 15$. The reversal potentials (in mV) are $E_K = -75$, $E_{Na} = 60$, $E_{Ca} = 80$, and $E_L = -60$. The applied currents (in $\mu$A/cm$^2$) are $I_s = -0.5$

and $I_d = 0$. The capacitance was $C_m = 3 \, \mu\text{F/cm}^2$ and the proportion of soma area was $p = 0.5$. We used non-bursting parameters for simplicity and the values of these parameters are based on the Pinsky-Rinzel model.

## B: GABAergic FS interneurons

We employed the Wang-Buzsáki model for the interneurons, a single compartment model with a sodium and a potassium channel [18]. The equation for the potential is

$$C_m \frac{dV_{fs}}{dt} = -I_{Na} - I_K - I_L - I_{syn,fs} + I_{fs}, \tag{8}$$

where the current are

$$\begin{aligned}
I_{Na} &= g_{Na} m_\infty^3 (V_{fs}) h (V_{fs} - E_{Na}), \\
I_K &= g_K n^4 (V_{fs} - E_K), \\
I_L &= g_L (V_{fs} - E_L).
\end{aligned} \tag{9}$$

The kinetic variables $h$ and $n$ obey eq.5, and the rate constants are given by

$$\begin{aligned}
\alpha_m &= \frac{-0.1(V_{fs} + 35)}{\exp(-0.1(V_{fs} + 35)) - 1}, \\
\beta_m &= 4 \exp(-(V_{fs} + 60)/18), \\
\alpha_h &= 0.07 \exp(-(V_{fs} + 58)/20), \\
\beta_h &= \frac{1}{\exp(-0.1(V_{fs} + 28)) + 1}, \\
\alpha_n &= \frac{-0.01(V_{fs} + 34)}{\exp(-0.1(V_{fs} + 34)) - 1}, \\
\beta_n &= 0.125 \exp(-(V_{fs} + 44)/80).
\end{aligned} \tag{10}$$

The kinetic variable $m$ was approximated by its asymptotic value $m_\infty(V) = \alpha_m/(\alpha_m + \beta_m)$. Other parameters for interneurons are fixed to standard values: the maximal conductances (in mS/cm$^2$) are $g_{Na} = 35$, $g_K = 9$, and $g_L = 0.1$; the reversal potentials (in mV) are $E_{Na} = 55$, $E_K = -90$, and $E_L = -65$; the membrane capacitance is $C_m = 1\ \mu$F/cm$^2$; and the applied current is $I_{fs} = 0\ \mu$A/cm$^2$.

## C: Synaptic connections

The set of synapses includes the synapse providing the external input. Their behavior is described by equations (11)-(17) below. When the voltage of a presynaptic cell goes beyond the fixed threshold, the synapse is activated and the postsynaptic cell receives excitation or inhibition. The synaptic currents in eq. (3) and (8) are given by

$$
\begin{aligned}
I_{syn,s} &= I_{GABA}, \\
I_{syn,d} &= I_{AMPA,rec} + I_{AMPA,ex} + I_{noise}, \\
I_{syn,fs} &= I_{AMPA,ei},
\end{aligned}
\tag{11}
$$

where

$$
\begin{aligned}
I_{GABA} &= g_{GABA}(V - E_{GABA}) \sum_{j=1}^{N_i} W_j^{ie} s_j^{GABA}, \\
I_{AMPA,rec} &= g_{AMPA,rec}(V - E_{AMPA}) \sum_{j=1}^{N_e} W_j^{ee} s_j^{AMPA,rec}, \\
I_{AMPA,ex} &= g_{AMPA,ex}(V - E_{AMPA}) s^{ex}, \\
I_{noise} &= g_{AMPA,n}(V - E_{AMPA}) s^{n}, \\
I_{AMPA,ei} &= g_{AMPA,ei}(V - E_{AMPA}) \sum_{n=1}^{N_e} W_j^{ei} s_j^{AMPA}.
\end{aligned}
\tag{12}
$$

Here $V$ is a membrane potential, and $s_j$ is a kinetic variable labeled by the index $j$ of a presynaptic neuron. We determined the connection matrices in the following way. Three memory patterns are independently embedded into the recurrent excitatory connections between pyramidal cells $W^{ee}$ via a clipped Hebbian learning rule [21]. $W^{ee}$ are fixed in such a way during simulation.

$$
W_{ij}^{ee} = \begin{cases} \min(1, \sum_{\mu=1}^{3} \eta_i^\mu \eta_j^\mu) \in \{0, 1\} & i \neq j \\ 0 & i = j, \end{cases}
\tag{13}
$$

where $\eta_i^\mu$ is the $\mu$-th component in the memory pattern, each of which is encoded by a value 1 (firing state) or 0 (resting state).

Each component of the connection matrix from pyramidal cells to interneurons $W^{ei}$ also takes the value one or zero. Each interneuron receives synapses from four pyramidal cells, which are selected randomly from the whole pyramidal cell population. The elements of the connection matrix from interneurons to pyramidal cells $W^{ie}$ are assumed to be uniformly distributed between 0 and 1. We used a reversal potential of $E_{GABA} = -75$ mV for GABA$_A$ synapses, and $E_{AMPA} = 0$ mV for AMPA synapses. The synaptic conductances (in mS/cm$^2$) are $g_{AMPA,rec} = 0.036$, $g_{AMPA,ex} = 0.225$, $g_{AMPA,n} = 0.0045$, and $g_{AMPA,ei} = 0.1$.
The synaptic gating variables, $s^{AMPA,rec}$ and $s^{AMPA}$, for the AMPA synapses obey

$$
\frac{ds}{dt} = H(V_{pre} + 40) - \beta_e s,
\tag{14}
$$

where $V_{pre}$ is the presynaptic potential, $\beta_e = 0.5$ ms$^{-1}$ is a decay rate, and is the Heaviside function

$$H(x) = \begin{cases} 1 & x > 0 \\ 0 & x \le 0. \end{cases} \tag{15}$$

The synaptic gating variables, $s^{ex}$ and $s^n$, for the AMPA synapse obey

$$\frac{ds}{dt} = \sum_k \delta(t - t^k_{poisson}) - \beta_e s, \tag{16}$$

where $t^k_{poisson}$ is $k$-th time of spike in a Poisson spike train. Each spike train is independently generated by a Poisson process with 100Hz firing rate in average for external inputs and 1kHz firing rate for background noise. The synaptic gating variable $s^{GABA}$ for the GABA$_A$ synapse obeys

$$\frac{ds}{dt} = \alpha_i F(V_{pre})(1 - s) - \beta_i s,$$
$$F(V_{pre}) = 1/(\exp(-V_{pre}/2) + 1), \tag{17}$$

where $\alpha_i = 12$ ms$^{-1}$ and $\beta_i = 0.1$ ms$^{-1}$ are the rise and decay rates for the inhibitions to pyramidal cells. Numerical integration was performed with a fourth-order Runge-Kutta method using a 0.05 ms time step.

# Acknowledgments

# References

[1] Amari S (1972) *Characteristics of random nets of analog neuron-like elements*. IEEE Trans Syst Man Cybern SMC-2:643-653

[2] Anderson JA (1972) *A simple neural network generating an interactive memory*. Math Biosci 14:197-220

[3] Nakano K (1972) *Associatron - A model of associative memory*. Man Cybern SMC-2:380-388

[4] Hopfield JJ (1982) *Neural networks and physical systems with emergent collective computational abilities*. Proc Natl Acad Sci USA 79:2554-2558

[5] Amit DJ (1994) *The Hebbian paradigm reintegrated: local reverberations as internal representations*. Behav Brain Sci 18:617-626

[6] Tsuda I, Koerner E, Shimizu H (1987) *Memory dynamics in asynchronous neural networks*. Prog Theor Phys 78:51-71

[7] Tsuda I (1992) *Dynamic link of memories - chaotic memory map in nonequilibrium neural networks*. Neural Netw 5:313-326

[8] Colliaux D, Molter C, Yamaguchi Y (2009) *Working memory dynamics and spontaneous activity in a flip-flop oscillations network model with a Milnor attractor*. Cogn Neurodyn. 3:141-51

[9] Klausberger T, Marton LF, Baude A, Roberts JDB, Magill P, Somogyi P (2004) *Spike timing of dendrite-targeting bistratified cells during hippocampal network oscillations in vivo*. Nat Neurosci 7:41-47

[10] Somogyi P, Klausberger T (2005) *Defined types of cortical interneurone structure space and spike timing in the hippocampus*. J Physiol 562:9-26

[11] Klausberger T, Somogyi P (2008) *Neuronal diversity and temporal dynamics: the unity of hippocampal circuit operations*. Science 321:53-7

[12] Marr D (1982) *Vision: A computational investigation into the human representation and processing of visual information*. New York

[13] Lawrence, JJ (2008) *Cholinergic control of GABA release: emerging parallels between neocortex and hippocampus*. Trends Neurosci 31:317-327

[14] Toth K, Freund TF, Miles R (1997) *Disinhibition of rat hippocampal pyramidal cells by GABAergic afferents from the septum*. J Physiol 500:463-474

[15] Salgado H, Bellay T, Nichols JA, Bose M, Martinolich L et al (2007) *Muscarinic M2 and M1 receptors reduce GABA release by Ca2+ channel modulation through activation of PI3K/Ca2+ -independent and PLC/Ca2+ -dependent PKC*. J Neurophysiol 98:952-965

[16] Csicsvari J, Hirase H, Czurko A, Mamiya A, Buzsaki G (1999) *Oscillatory coupling of hippocampal pyramidal cells and interneurons in the behaving rat*. J Neurosci 19:274-287

[17] Pinsky PF, Rinzel J (1994) *Intrinsic and network rhythmogenesis in a reduced Traub model for CA3 neurons*. J Comput Neurosci 1:39-60

[18] Wang XJ, Buzsaki G (1996) *Gamma oscillation by synaptic inhibition in a hippocampal interneuronal network model*. J Neurosci 16:6402-6413

[19] Nara S, Davis P (1992) *Chaotic wandering and search in a cycle-memory neural network*. Prog Theor Phys 88:845-855

[20] Russo E, Treves A (2012) *Cortical free-association dynamics: Distinct phases of a latching network*. Phys Rev E. DOI 10.1103/PhysRevE.85.051920

[21] Willshaw D, Buneman O, Longuet-Higgins H (1969) *Non-holographic associative memory*. Nature 222:960-962